Percolation phenomenon in ternary microemulsions: The effect of pressure

C. Boned,[1] Z. Saidi,[1] P. Xans,[1] and J. Peyrelasse[2]
[1]*Laboratoire Haute Pression, Université de Pau, Centre Universitaire de Recherche Scientifique, Avenue de l'Université, 64000 Pau, France*
[2]*Laboratoire de Physique des Matériaux Industriels, Université de Pau, Centre Universitaire de Recherche Scientifique, Avenue de l'Université, 64000 Pau, France*
(Received 9 November 1993)

The electrical conductivity σ and dynamic viscosity η of water-based water-AOT-undecane [AOT:sodium bis(2-ethylhexyl) sulfosuccinate] microemulsions and waterless glycerol-AOT-isooctane microemulsions were studied as a function of volume fraction ϕ in dispersed matter (water plus AOT or glycerol plus AOT) and pressure up to 1000 bar. The realm of existence of the single-phase zone was also determined versus pressure P. The curves $\eta(P)$ and $\sigma(P)$ at constant ϕ and temperature T, and the curves $\eta(\phi)$ and $\sigma(\phi)$ at constant P and T were analyzed within the framework of percolation theory. For water-based microemulsions the percolation threshold ϕ_c decreases when P increases, corresponding to an increase in interactions. For waterless microemulsions ϕ_c varies very little. The scaling exponents are ≈ 2 above the threshold and ≈ -1.2 below, whatever the pressure, the system, and the property studied (values which have already between obtained at 1 bar). This corresponds to the fact that these systems belong to the same class of universality.

PACS number(s): 82.70.−y, 05.40.+j, 66.20.+d, 72.90.+y

I. INTRODUCTION

We recently published [1] a study concerning results obtained on electrical conductivity, dielectric relaxation (static permittivity and characteristic frequency), and dynamic viscosity for microemulsions with very varied compositions (water-based or waterless, ternary or quaternary, with or without salt). However, they do have in common the fact that they all correspond to the distribution model of spheres subjected to Brownian movement dispersed in a continuum. For all these systems the associated dynamic percolation model [2,3] is qualitatively verified. Moreover, when the conditions of application of the theory's asymptotic laws are satisfied the scaling exponents are the same for all systems (approximately 2 above the threshold and -1.2 below it), which is consistent with the theoretical predictions. This reflects the fact that all these systems belong to the same class of universality. We also showed [4] that for correct and convenient study of the phenomenon of percolation it is essential to choose an appropriate experimental path which does not affect interactions. Other paths are of course possible, since if one begins with a system located below the percolation threshold ϕ_c (ϕ: volume fraction in dispersed matter) it is not absolutely necessary to change ϕ in order to reach the threshold. One can for example vary the temperature, but we have shown [5,6] that this makes analysis of the curves difficult as the experimental path followed no longer maintains constant interactions. Correct analysis requires the introduction into these conditions (constant ϕ and variable T) of a percolation temperature T_c such that $\phi_c(T_c)=\phi$. Moreover, at constant ϕ and T the salinity p of the system can be varied and a percolation salinity p_c introduced or one can vary the molar ratio [water]/[surfactant], etc. All these studies as well as most of those published by a number of other authors (for example, Refs. [7]–[10]) connected with percolation in microemulsions were carried out at atmospheric pressure.

In this paper we will consider another experimental pathway whereby interactions can be varied in the system to move it closer to or farther from the percolation threshold, i.e., the pathway based on varying pressure. Recent studies [11] have shown that temperature and pressure can be used to control the stability of microemulsions. Light scattering and SANS (small angle neutron scattering) measurements were made as a function of pressure [12,13] for the water-AOT-oil systems [AOT: sodium bis (2-ethylhexyl) sulfosuccinate]. It was shown that at fixed temperature, when pressure increases the microemulsion becomes opaque at it approaches a certain limit and phase separation takes place. The presence of a very large cluster of droplets with strong interdroplet attraction was suggested. Moreover, SANS measurements [12] show that pressure variation (and hence density variation) has no measurable effect on the radius of droplets in the single-phase domain. In a review article [14] it is stated that the effect of pressure is similar to that of temperature in that it controls the phase separation limit. Thus when the phase boundary is approached as a result of varying pressure (or temperature) the pairwise droplet attraction becomes enhanced but the water radius is not affected. Invariability of size has also been observed in other studies [15].

At this stage it is interesting to mention a recent study [16] on pressure effects on the phase behavior of a propylene-water-surfactant mixture. The effect of increasing pressure is similar to the effect of reducing temperature or increasing the electrolyte concentration, in agreement with a phenomenological model [17]

developed for the phase behavior of amphiphile-water-oil systems.

The conductivities of the nominally propylene-continuous upper phases in the systems are high enough to suggest electrical percolation, implying the presence of significant volume fractions of micelles in these phases. The upper phases also present high viscosity. However the phenomenon of percolation as such was not studied specifically. It is important to recall another recent study [18] on micellar and bicontinuous microemulsions formed in both near-critical and super-critical propane with didodecyldimethylammonium bromide (DDAB) and water. The phase behavior of this system presents unusual and dramatic effects due to pressure. When the pressure of the system is increased from 80–400 bar, the conductivity is observed to decrease by three orders of magnitude. This conductivity effect appears to be consistent with a change in the microstructure (structural change from interconnected conduits to dispersed droplets). The authors refer to an "antipercolation" effect. As regards our own work as reported in this paper, we will consider those systems for which we have already verified [4,6,19] that they present a highly marked percolation effect at atmospheric pressure. These systems were studied at various pressures.

II. EXPERIMENTAL TECHNIQUES

Our experimental measurements were concerned with determining dynamic viscosity η, electrical conductivity σ and density ρ versus pressure P, and volume fraction ϕ at a given temperature T. The value of the viscosity η is determined by means of a falling body viscometer which operates at up to 4000 bar and whose characteristics are specified in detail elsewhere [20]. The density ρ is measured by means of a DMA 45 ANTON PAAR KG densimeter to which the additional DMA 512 cell has been added, enabling measurements to be made up to 400 bar. Use of this apparatus with a double reference calibration system was the subject of another article in a specialized journal [21]. Beyond 400 bar the values of ρ are extrapolated according to the method described in an earlier paper [22]. This shows that the relative uncertainty on the values of ρ determined in this way has practically no influence on the relative uncertainty of the viscosity η which can be estimated as being of the order of 2% for $P \leq 1000$ bar. The electrical conductivity σ is measured with the aid of a semiautomatic Wayne-Kerr B331 measuring bridge operating at a frequency of 1591.5 Hz (pulsation 10^4 rad sec^{-1}). The pressure measurement cell manufactured in the laboratory [23] allows measurements at up to 1500 bar. For all of these devices one has $\Delta P = 0.5$ bar (at pressures other than atmospheric pressure). For the viscometer $\Delta T = 0.5\,^{\circ}$C, while for the densimeter and conductivimeter $\Delta T = 0.1\,^{\circ}$C.

We studied on the one hand the waterless microemulsions glycerol-AOT-isooctane and on the other hand the water-based microemulsions water-AOT-undecane. The substances used were distilled water, glycerol (Aldrich purity >99%), AOT (Sigma purity >99%), isooctane (Fluka purity >99.5%), and undecane (Fluka purity >99%). The samples at given P and T are characterized by the volume fraction ϕ in dispersed matter (water plus AOT or glycerol plus AOT) and by the molar ratio n ([water]/[AOT] or [glycerol]/[AOT]). We will see below that because of the influence of pressure on the density of the components, for a given system ϕ varies slightly with pressure. We will therefore use ϕ_0 to denote the volume fraction at 1 bar. Finally the measurements were generally carried out at $T = 25\,^{\circ}$C for waterless microemulsions and $T = 20\,^{\circ}$C for water-based microemulsions, because these systems had previously been studied [4,6,19] at these temperatures and at atmospheric pressure.

III. STUDY OF PHASE DIAGRAM BEHAVIOR WITH PRESSURE

We first examined the behavior of phase diagrams under pressure of the samples studied, with a view to identifying accurately the realm of existence of the single-phase zone. To do this we used a ROP brand full visibility sapphire cell, details of which can be found in the literature [24]. It can be used to carry out measurements at pressures up to 500 bar. The sample is subjected to an isothermal pressure variation and the liquid-liquid transition is clearly identifiable since the fluid becomes opaque and scatters light to a considerable extent.

A. Glycerol-AOT-isooctane system

Figure 1 represents the realm of existence of the single-phase zone in the plane (P, T) for the microemulsion of molar ratio $n = 4$, such that $\phi_0 = 0.20$ at 25 °C. It is seen to remain single phase all along the $T = 25\,^{\circ}$C isotherm, and this is also the case with this system for other values of ϕ_0. Figure 1 shows that for temperatures above 34 °C the system moves from a two-phase domain to a single-phase domain under the effect of pressure. In other words the single phase of the domain of the microemulsion increases (at given ϕ_0) with increasing pressure.

B. Water-AOT-undecane system

Figure 2 represents the realm of existence of the single-phase zone in the (P, T) plane for the microemul-

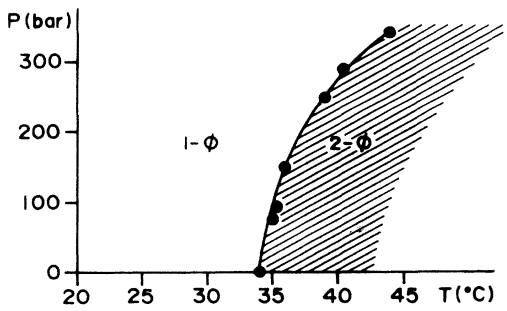

FIG. 1. Realm of existence of the single-phase zone. Glycerol-AOT-isooctane system. (Molar ratio $n = 4$, volume fraction at 1 bar $\phi_0 = 0.20$, $T = 25\,^{\circ}$C.) 1ϕ, one-phase area; 2ϕ, two-phase area.

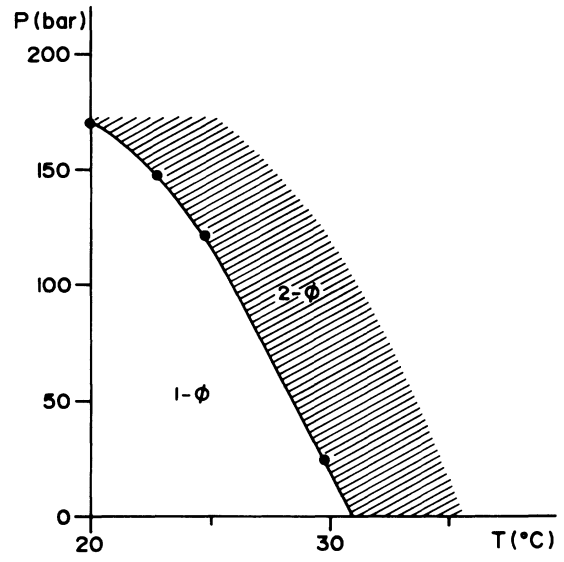

FIG. 2. Realm of existence of the single-phase zone. Water-AOT-undecane system. (Molar ratio $n=30$, volume fraction at 1 bar $\phi_0=0.20$, $T=20$ °C.) 1ϕ, one-phase area; 2ϕ, two-phase area.

sion of molar ratio $n=30$ such that $\phi_0=0.20$ at 20 °C. With the sapphire cell, we determined the boundary pressure $P=161$ bar at 20.2 °C, at which the transparent system changes into an opaque system. It will be observed that the water-AOT-undecane system has a domain which shrinks with increasing pressure, an observation which had already been made [11] for the similar water-AOT-octane systems. For water-hexadecyltrimethyl ammonium bromide (CTAB)-chloroform-heptane systems, on the other hand, the domain increases [11] as it does with the glycerol-AOT-isooctane system.

IV. EXPERIMENTAL RESULTS ON CONDUCTIVITY AND VISCOSITY

Taking account of all our previous results at $P=1$ bar we know that the percolation phenomenon is clearly visible with viscosity η for the glycerol-AOT-isooctane system and with electrical conductivity σ for the water-AOT-undecane system.

A. Study of the viscosity η

We first studied variations of η versus P for a given sample. Figure 3 represents variations of $\eta(P)$ for $n=4$, $T=25$ °C, and $\phi_0=0.30$. An increase in η was observed. Figure 4 represents variations of $\log_{10}\eta$ versus P for $n=4$, $T=25$ °C, and several values of ϕ_0. Variations of pure glycerol and pure isooctane are also represented. We also carried out measurements at constant pressure as a function of the volume fraction ϕ_P, which is the real volume fraction at the pressure P considered, calculated from ϕ_0 on the basis of variations versus pressure of densities of components [Figs. 5(a) and 6(a)]. The sigmoid shape of the curves for $\log_{10}\eta$ versus ϕ_P at $P=C^{te}$ will be

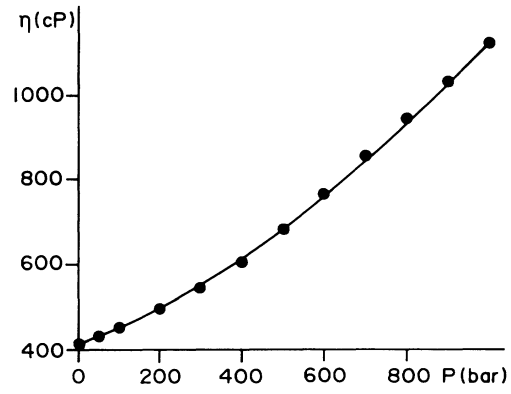

FIG. 3. Glycerol-AOT-isooctane system. Variations of η vs P. (Molar ratio $n=4$, volume fraction at 1 bar $\phi_0=0.30$, $T=25$ °C.)

observed. It will be noted that the interval of variation extends over approximately three decades.

B. Study of the electrical conductivity σ

Figure 7 represents for the water-AOT-undecane system ($T=20$ °C, $n=30$, $\phi_0=0.15$) the curves for variations of σ versus P, while Fig. 8 represents the curves for variations of $\log_{10}\sigma$ versus P for several values of Φ_0. Figures 9(a) and 10(a) represent for the same system the curves for variations of $\log_{10}\sigma$ versus ϕ_P for 50 and 150 bar. Here again the sigmoid shape of the curves and the large interval of the variations (approximately 5 decades) can be observed.

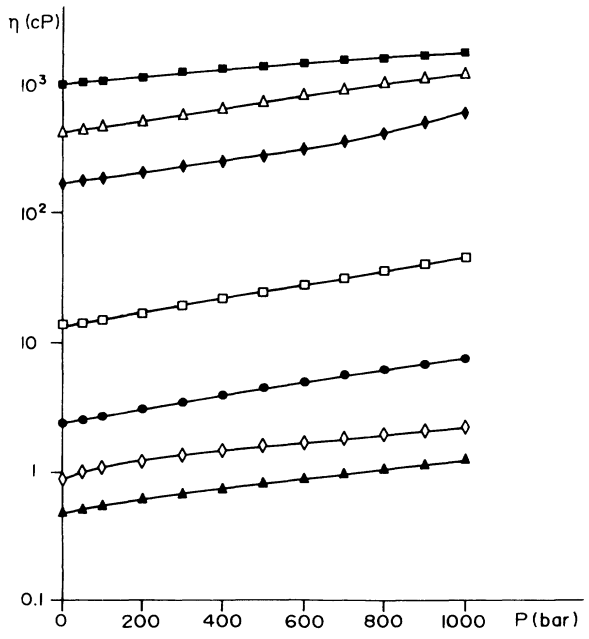

FIG. 4. Glycerol-AOT-isooctane system. Variations of $\log_{10}\eta$ vs P, for several values of the volume fraction ϕ_0 at 1 bar. (Molar ratio $n=4$, $T=25$ °C.) △, 0.30; ♦, 0.25; □, 0.15; ●, 0.10; ◇, 0.064; ■, glycerol; ▲, isooctane.

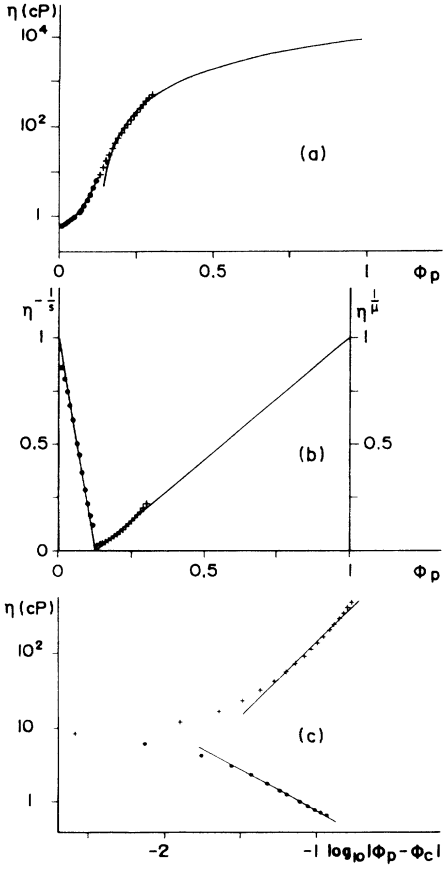

FIG. 5. Glycerol-AOT-isooctane system. (Molar ratio $n=4$, $T=25\,°C$, $P=200$ bar.) (a) Variations of $\log_{10}\eta$ vs ϕ_P. +, experimental points; –, theoretical curve. (b) Variations of $\eta^{1/\mu}$ and $\eta^{-1/s}$ vs ϕ_P. (Values normalized to 1 for $\phi_P=0$ and $\phi_P=1$.) +, experimental points; –, theoretical curve. (c) Variations of $\log_{10}\eta$ vs $\log_{10}|\phi_P-\phi_c|$. +, experimental points; –, theoretical curve.

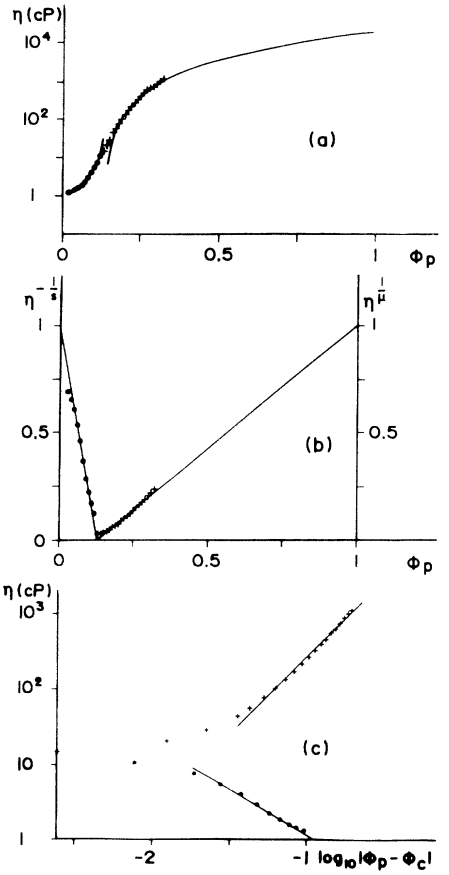

FIG. 6. Glycerol-AOT-isooctane system. (Molar ratio $n=4$, $T=25\,°C$, $P=1000$ bar.) (a) Variations of $\log_{10}\eta$ vs ϕ_P. +, experimental points; –, theoretical curve. (b) Variations of $\eta^{1/\mu}$ and $\eta^{-1/s}$ vs ϕ_P. (Values normalized to 1 for $\phi_P=0$ and $\phi_P=1$.) +, experimental points; –, theoretical curve. (c) Variations of $\log_{10}\eta$ vs $\log_{10}|\phi_P-\phi_c|$. +, experimental points; –, theoretical curve.

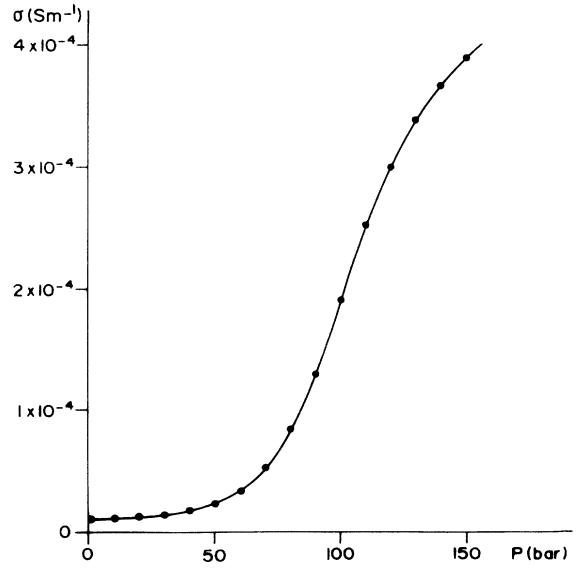

FIG. 7. Water-AOT-undecane system. Variations of σ vs P. (Molar ratio $n=30$, volume fraction at 1 bar $\phi_0=0.15$, $T=20\,°C$.)

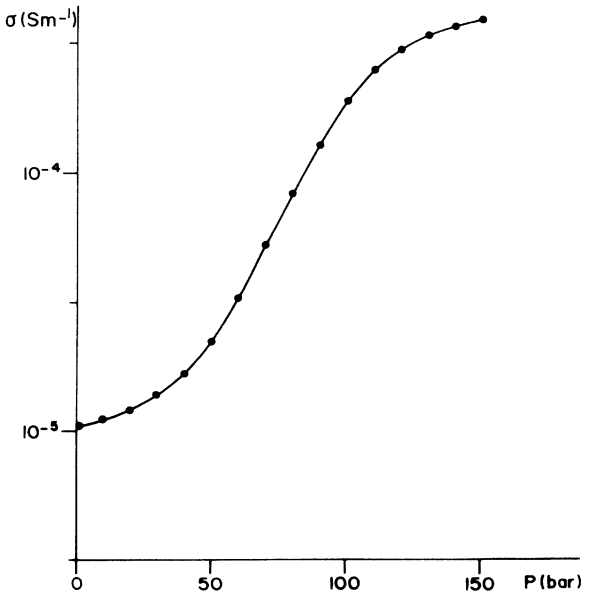

FIG. 8. Water-AOT-undecane system. Variations of $\log_{10}\sigma$ vs P. (Molar ratio $n=30$, volume fraction at 1 bar $\phi_0=0.15$, $T=20\,°C$.)

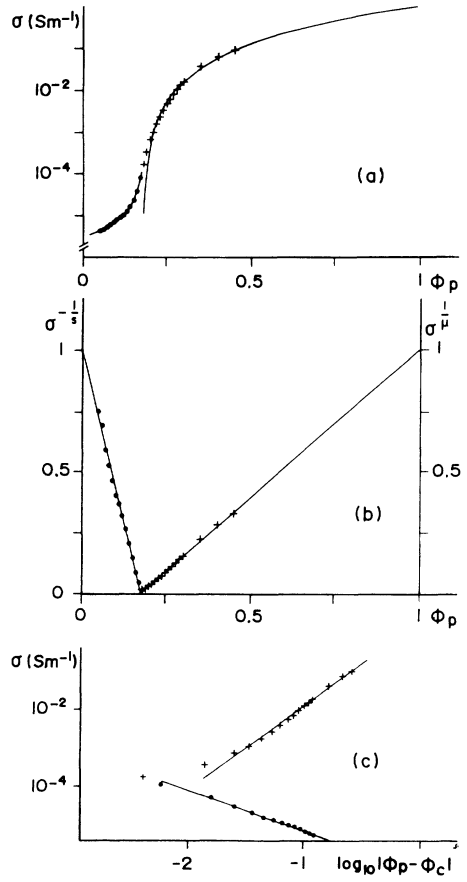

FIG. 9. Water-AOT-undecane system. (Molar ratio $n=30$, $T=20\,^{\circ}\mathrm{C}$, $P=50$ bar.) (a) Variations of $\log_{10}\sigma$ vs ϕ_P. +, experimental points; –, theoretical curve. (b) Variations of $\sigma^{1/\mu}$ and $\sigma^{-1/s}$ vs ϕ_P. (Values normalized to 1 for $\phi_P=0$ and $\phi_P=1$.) +, experimental points; –, theoretical curve. (c) Variations of $\log_{10}\sigma$ vs $\log_{10}|\phi_P-\phi_c|$. +, experimental points; –, theoretical curve.

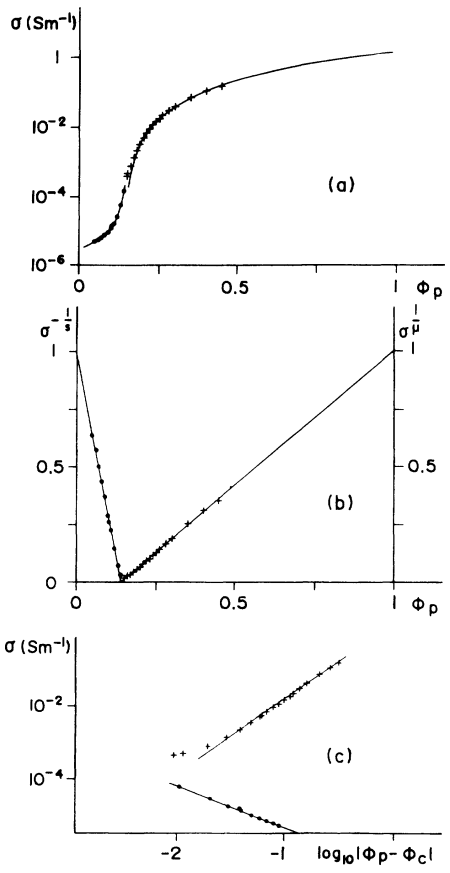

FIG. 10. Water-AOT-undecane system. (Molar ratio $n=30$, $T=20\,^{\circ}\mathrm{C}$, $P=150$ bar.) (a) Variations of $\log_{10}\sigma$ vs ϕ_P. +, experimental points; –, theoretical curve. (b) Variations of $\sigma^{1/\mu}$ and $\sigma^{-1/s}$ vs ϕ_P. (Values normalized to 1 for $\phi_P=0$ and $\phi_P=1$.) +, experimental points; –, theoretical curve. (c) Variations of $\log_{10}\sigma$ vs $\log_{10}|\phi_P-\phi_c|$. +, experimental points; –, theoretical curve.

V. DISCUSSION OF RESULTS

A. Theoretical background

Analysis of earlier studies carried out on percolation indicates that the following relationships can be adopted as asymptotic laws of behavior. It is generally assumed that the system is made up of two components (1) and (2) and that ϕ is the volume fraction of component (1),

$$\phi>\phi_c+\delta,\quad \sigma=C_1\sigma_1(\phi-\phi_c)^{\mu},\quad \eta=C_1'\eta_1(\phi-\phi_c)^{\mu},$$
$$\phi<\phi_c-\delta',\quad \sigma=C_2\sigma_2(\phi_c-\phi)^{-s},\quad \eta=C_2'\eta_2(\phi_c-\phi)^{-s}, \tag{1}$$

in which $\Delta=\delta+\delta'$ is the width of the transition interval (the "crossover regime") which is of the order of $\Delta_\sigma=(\sigma_2/\sigma_1)^{1/(\mu+s)}$ for conductivity [25]. These relationships indicate that the derivatives $(1/\sigma)(d\sigma/d\phi)$ and $(1/\eta)(d\eta/d\phi)$ tend towards infinity at the percolation threshold ϕ_c. In fact, experimentally, there is a continuous transition in the transition interval Δ in the immediate neighborhood of ϕ_c and $(1/\sigma)(d\sigma/d\phi)$, and $(1/\eta)(d\eta/d\phi)$ goes through a maximum at the threshold. At $P=1$ bar, a very close adjustment of conductivity of the water-AOT-undecane system is obtained [19] between the experimental curves and the theoretical values, using $\mu=1.94$ and $s=1.2$, which clearly reflects the dynamic aspect of the phenomenon [2,3]. Quantitative analysis performed on the viscosity of waterless microemulsions gives [26,27] $\mu=2.00\pm0.25$ and $s=1.2\pm0.2$. In both cases, (conductivity and viscosity) the scaling exponents at $P=1$ bar are practically identical, which shows that these microemulsions, which are very different in their compositions, behave in a very similar way as regards dynamic percolation, provided the conditions of application of the asymptotic laws are satisfied [1].

B. Analysis of the results

The $\log_{10}\eta=f(\phi_P)$ curves at given pressure have a sigmoid shape which merits analysis. To do this the coefficients of a fourth degree polynomial in ϕ_P were adjusted in the most sharply increasing part of the curve

and the value of ϕ_P for which the second derivative of this polynomial is cancelled out was identified. This value is that of the point of inflexion, in other words, of the maximum for $(1/\eta)(d\eta/d\phi_P)$. It corresponds to the position of the percolation threshold ϕ_c. As an illustration, Fig. 11 represents the variations of $(1/\eta)(d\eta/d\phi_P)$ versus ϕ_P at $P=200$ bar (glycerol-AOT-isooctane system, $n=4$, $T=25\,^\circ$C) in which the points correspond to the numerical derivative and in which the solid line corresponds to the polynomial obtained after adjustment of experimental $\log_{10}\eta$ values. Once ϕ_c has been ascertained, the least squares method is used to adjust the theoretical expressions [Eqs. (1)] in such a way as to be able to determine the exponents μ and s. For all the pressures studied, 1, 50, 100, 200, 400, 600, 800, and 1000 bar, we found $1.855<\mu<2.048$ and $1.029<s<1.211$ with mean values $\mu=1.914$ and $s=1.108$. Figures 5(a) and 6(a) represent the experimental and theoretical $\log_{10}\eta$ curves for $P=200$ bar and $P=1000$ bar. We also show in Figs. 5(b) and 6(b) the variations of $\eta^{1/\mu}$ and $\eta^{-1/s}$ as a function of ϕ_P normalizing to 1 for $\phi_P=0$ and $\phi_P=1$. Finally, Figs. 5(c) and 6(c) represent variations of $\log_{10}\eta$ versus $\log_{10}|\phi_P-\phi_c|$. For all three types of representation the excellent fit between experimental values and theoretical curves [Eqs. (1)] will be observed. It will be noted that representations 5(a), 5(c), 6(a), and 6(c) clearly show the existence of a transition interval Δ_η when $\phi_P\rightarrow\phi_c$. Finally, Fig. 12 represents variations of ϕ_c versus P ($n=4$, $T=25\,^\circ$C). It will be seen that ϕ_c is practically constant with perhaps a slight decrease when P increases. This result should be linked to the fact that as $P=1$ bar, ϕ_c also varies little when the temperature increases [5,6], reflecting the fact that the interactions change little in this system.

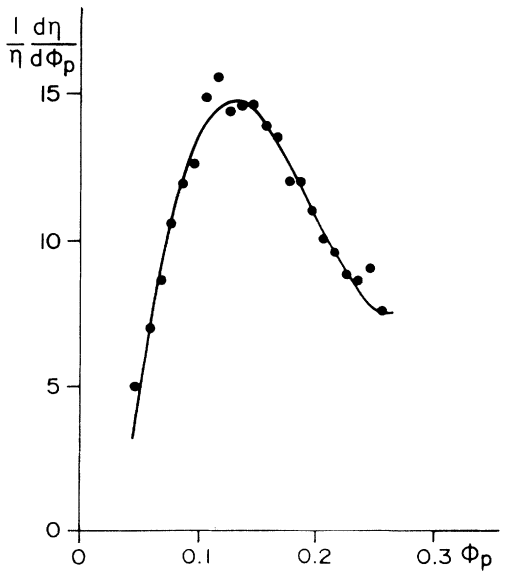

FIG. 11. Glycerol-AOT-isooctane system. Variations of $(1/\eta)(d\eta/d\phi_P)$ vs ϕ_P. (Molar ratio $n=4$, $T=25\,^\circ$C, $P=200$ bar.) ●, numerical derivative;–, adjustment polynomial. (The maximum corresponds to the percolation threshold.)

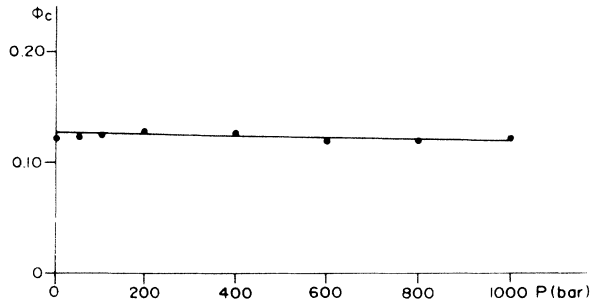

FIG. 12. Water-AOT-isooctane system. (Molar ratio $n=4$, $T=25\,^\circ$C.) Variations of the percolation threshold ϕ_c vs pressure P.

We proceeded in the same way for the water-based microemulsions water-AOT-undecane ($n=30$) for the study of electrical conductivity σ. Figure 13 represents variations of $(1/\sigma)(d\sigma/d\phi_P)$ versus ϕ_P for $P=150$ bar. We also determined ϕ_c for $P=1$, 50, 100, and 150 bar. Then numerical analysis of experimental values of σ gives $2.110<\mu<2.252$ and $1.05<s<1.36$ with mean values $\mu=2.166$ and $s=1.172$. Figures 9(a) and 10(a) represent values of $\log_{10}\sigma$ versus ϕ_P for $P=50$ bar and $P=150$ bar. Figures 9(b) and 10(b) correspond to $\sigma^{1/\mu}$ and $\sigma^{-1/s}$ versus ϕ_P (normalized to 1 for $\phi_P=0$ and 1). Finally Figs. 9(c) and 10(c) correspond to variations of $\log_{10}\sigma$ versus $\log_{10}|\phi_P-\phi_c|$. Here again the excellent fit between experimental values and theoretical curves will be noted, as will the existence of the transition interval Δ_σ

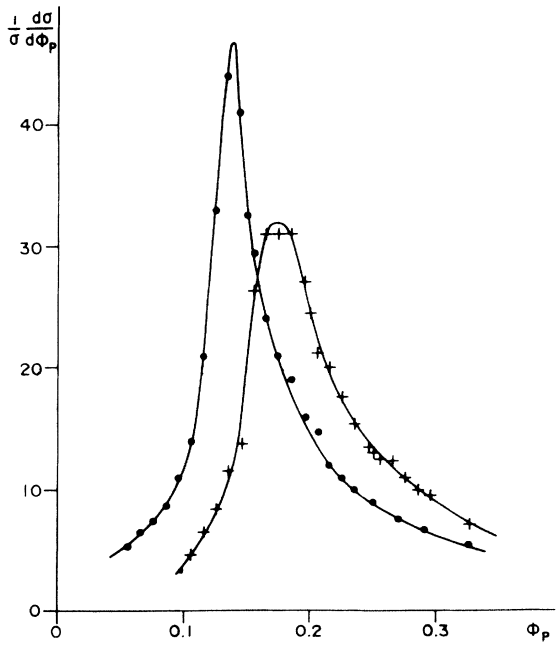

FIG. 13. Water-AOT-undecane system. Variation of $(1/\sigma)(d\sigma/d\phi_P)$ vs ϕ_P. (Molar ratio $n=30$, $T=20\,^\circ$C.) ●, numerical derivative ($P=150$ bar); +, numerical derivative ($P=50$ bar); –, adjustment polynomial. (Maxima correspond to the percolation thresholds.)

[Figs. 9(a), 10(a), 9(c), and 10(c)] in the immediate neighborhood of ϕ_c. Finally, Fig. 14 represents variations of ϕ_c versus P. It will be observed that for water-based microemulsions, ϕ_c decreases markedly with increasing pressure. This result should be linked to the sharp decrease in ϕ_c versus T observed for identical [19] or similar [9] systems at $P=1$ bar, which reflects an increase in interactions.

Figures 12 and 14 show that, depending on the system, ϕ_c may or may not be a function of the pressure P. In Eqs. (1) the quantities σ_1, σ_2, η_1, η_2 on the one hand, and the prefactors C_1, C_1', C_2, C_2' on the other hand are *a priori* functions of P. For example, for isooctane at 25 °C one obtains $\eta=0.472$ cP at 1 bar and 1.235 cP at 1000 bar, and for glycerol at the same temperature one obtains 955 cP at 1 bar and 1680 cP at 1000 bar. However, if, for varying P, $\phi_c(P)$ remains in the neighborhood of the value ϕ_P, one can write, developing to the first order, $\phi_c(P)=\phi_P+K(P-P_c)$ in which $K=(d\phi_c/dP)_{P_c}$ and $\phi_c(P_c)=\phi_P$, which defines the percolation pressure P_c. If $K<0$, which corresponds to the case in Fig. 14, then $\phi_c>\phi_P$, if $P>P_c$, and this implies the following relationships:

$$\sigma=C_1(P)\sigma_1(P)[K(P_c)(P_c-P)]^{\mu} \text{ if } P>P_c+\delta_P ,$$
$$\sigma=C_2(P)\sigma_2(P)[K(P_c)(P-P_c)]^{-s} \text{ if } P<P_c-\delta_P' . \quad (2)$$

These relationships are not valid in the immediate neighborhood of P_c (in other words, ϕ_c) where there is continuous variation in a narrow pressure interval around the percolation threshold P_c. The cross-over regime is $\Delta_P=\delta_P+\delta_P'$. One thus has scaling laws for variations of σ (and also of η) versus P with the same exponents μ and s as for variations of σ (and also for η) versus ϕ. It has also already been shown [5,26] that one also has the same exponents at constant ϕ and P for variations versus temperature T. But it is essential to emphasize that analysis of variations of σ and η with Eqs. (2) (or similar for η) is only simple if K is independent of P_c and if σ_1, σ_2, η_1, η_2, C_1, C_1', C_2, C_2' are also independent of P, which is not generally the case. Moreover, as we have already indicated, there is also a small variation in the volume fraction ϕ_P of the sample when pressure varies, this variation being due to the influence of pressure on the system components's density. For example at $T=25$ °C the values obtained for isooctane are $\rho=0.6874$ g/cm^3 at 1 bar and 0.7627 g/cm^3 at 1000 bar. For glycerol, the results are respectively 1.2546 g/cm^3 and 1.2856 g/cm^3. Assuming that the density of AOT varies very little, if at $P=1$, bar one has $\phi_0=0.15$, then at 1000 bar one has $\phi_P=0.163$ ($n=4$, $T=25$ °C). Similarly, if $\phi_0=0.30$ then one obtains $\phi_P=0.320$ at 1000 bar. For the water-AOT-undecane systems pressure variations are less marked and so the value of ϕ varies little. For example, if $\phi_0=0.301$ then $\phi_P=0.303$ at 150 bar ($n=30$, $T=20$ °C). The result is that in fact, for any given sample, the value P_c of the threshold for that sample is itself a function of pressure because one has $\phi(P)$. However this variation only has any influence when the pressure is such that the sample is close to the percolation threshold. It is only if all these effects are negligible (which is not the case here because of the variations of η_1, η_2, σ_1, σ_2 versus pressure) that $\log_{10}\sigma=f(\log_{10}|P-P_c|)$ or $\log_{10}\eta=f(\log_{10}|P-P_c|)$ corresponds to two straight lines of slopes μ and $-s$.

If, as is the case here, these effects are not negligible, it is difficult or even impossible to determine experimentally the values of μ and s with this experimental pathway (variable P) and, in general, satisfactory analysis of the experimental curves is complicated. Figures 3 and 4 for viscosity and Figs. 7 and 8 for conductivity, which represent variations as a function of P for a given system [ϕ_0 imposed, but $\phi(P)$], are characteristic of this difficulty. Let us recall that the same is true for the experimental pathway which consists in variable temperature T, which can produce curious effects [5,6] that are difficult to analyze unless certain precautions are taken.

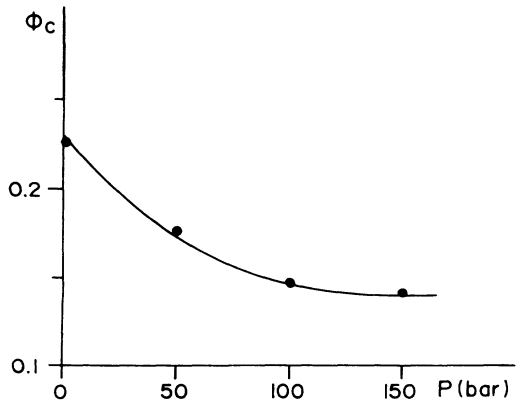

FIG. 14. Water-AOT-undecane system. (Molar ratio $n=30$, $T=20$ °C.) Variations of the percolation threshold ϕ_c vs pressure P.

VI. CONCLUSION

The two ternary systems considered here correspond to a dispersion of spheres in a continuum, the spheres being subjected to Brownian movement. The dynamic description of the phenomenon of percolation applies and the theoretical predictions are verified, whatever the pressure, both the conductivity σ and the viscosity η increase with the content of dispersed matter ϕ [with $(1/\sigma)(d\sigma/d\phi)$ and $(1/\eta)(d\eta/d\phi)$ passing through a maximum as a function of ϕ]. Quantitatively, it is very satisfying to observe that when the conditions of application of the asymptotic laws of the theory are satisfied, the scaling exponents are the same, i.e., ≈ 2 above the threshold and ≈ -1.2 below the threshold whatever the system, the property studied, and the pressure. This indicates that the systems belong to the same class of universality. For the water-AOT-undecane systems we observed that the percolation threshold decreases with increasing pressure, thus reflecting an increase in interactions. It has recently been possible [9,28,29] to calculate quantitatively the variations of ϕ_c versus T solely on the basis of knowledge of variations of interactions versus T. It would be interesting to apply this model to variations of pressure.

In an earlier article [4] we insisted on the importance of the experimental pathway. In the present study we chose to vary pressure while maintaining the other parameters constant. Equations (2) show that the distance $|\phi(P)-\phi_c(P)|$ is essential. As the threshold varies at each point on the pathway it is possible to pass through a percolation point which defines the percolation pressure P_c. As the prefactors (and also ϕ) of the asymptotic equations are also dependent on P, this makes correct analysis of the experimental curves $\eta(P)$ or $\sigma(P)$ substantially more difficult. This illustrates the difficulty of interpreting experimental data when the phenomenon of percolation is involved, and the importance of accurately controlling all the parameters when one experimental pathway has been selected. Unless this is done there is a direct risk of arriving at faulty interpretations.

[1] C. Boned, J. Peyrelasse, and Z. Saidi, Phys. Rev. E **47**, 468 (1993).
[2] M. Lagues, J. Phys. Lett. (Paris) **40**, L331 (1979).
[3] G. S. Grest, J. Webman, S. A. Safran, and A. Bug, Phys. Rev. A **33**, 2842 (1986).
[4] J. Peyrelasse and C. Boned, Phys. Rev. A **41**, 938 (1990).
[5] Z. Saidi, C. Boned, and J. Peyrelasse, Prog. Colloid Polym. Sci. **89**, 156 (1992).
[6] C. Mathew, Z. Saidi, J. Peyrelasse, and C. Boned, Phys. Rev. A **43**, 873 (1991).
[7] M. A. Van Dijk, Phys. Rev. Lett. **55**, 1003 (1985).
[8] S. Bhattacharya, J. P. Stokes, M. W. Kim, and J. S. Huang, Phys. Rev. Lett. **55**, 1884 (1985).
[9] C. Cametti, P. Codastefano, P. Tartaglia, S. H. Chen, and J. Rouch, Phys. Rev. A **45**, R5358 (1992).
[10] M. W. Kim and J. S. Huang, Phys. Rev. A **34**, 719 (1986).
[11] J. Eastoe, B. H. Robinson, and D. C. Steyler, J. Chem. Soc. Faraday Trans. **86**, 511 (1990).
[12] J. Eastoe, W. K. Young, B. H. Robinson, and D. C. Steytler, J. Chem. Soc. Faraday Trans. **86**, 2883 (1990).
[13] R. D. Smith, J. P. Blitz, and J. L. Fulton, ACS Symp. Ser. **406** (Super Crit. Fluid Sci. Technol.), 165 (1989).
[14] J. Eastoe, B. H. Robinson, D. C. Steytler, and D. Thorn-Leeson, Adv. Colloid Interface Sci. **36**, 1 (1991).
[15] E. W. Kaler, J. F. Billman, J. L. Fulton, and R. D. Smith, J. Phys. Chem. **95**, 458 (1991).
[16] E. J. Beckman and R. D. Smith, J. Phys. Chem. **95**, 3253 (1991).
[17] M. Kahlweit, M. Strey, R. Schomacker, and D. Haase, Langmuir **5**, 305 (1989).
[18] J. M. Tingey, J. L. Fulton, D. W. Matson, and R. D. Smith, J. Phys. Chem. **95**, 1445 (1991).
[19] M. Moha-Ouchane, J. Peyrelasse, and C. Boned, Phys. Rev. A **35**, 3027 (1987).
[20] D. Ducoulombier, F. Lazarre, H. Saint-Guirons, and P. Xans, Rev. Phys. Appl. **20**, 735 (1985).
[21] B. Lagourette, C. Boned, H. Saint-Guirons, P. Xans, and H. Zhou, Meas. Sci. Technol. **3**, 699 (1992).
[22] M. Kanti, H. Zhou, S. Ye, C. Boned, B. Lagourette, H. Saint-Guirons, P. Xans, and F. Montel, J. Phys. Chem. **93**, 3860 (1989).
[23] Z. Saidi, C. Boned, P. Xans, and J. Peyrelasse, 7th European Colloid and Interface Society Congress, Bristol, 1993, Prog. Colloid Polym. Sci. (to be published).
[24] J. L. Daridon, H. Saint-Guirons, B. Lagourette, and P. Xans, High Pressure Res. **9**, 309 (1992).
[25] A. L. Efros and B. L. Shklovskii, Phys. Status Solidi B **76**, 475 (1976).
[26] C. Boned and J. Peyrelasse, J. Surf. Sci. Technol. **7**, 1 (1991).
[27] Z. Saidi, C. Mathew, J. Peyrelasse, and C. Boned, Phys. Rev A **42**, 872 (1990).
[28] J. Peyrelasse, C. Boned, and Z. Saidi, Phys. Rev. E **47**, 3412 (1993).
[29] C. Cametti, P. Codastefano, P. Tartaglia, J. Rouch, and S. H. Chen, Phys. Rev. Lett. **64**, 1461 (1990).